DEEP LEARNING FOR SUPER-RESOLUTION OF SEA ICE CONCENTRATION: CASE STUDY OF OSISAF DOWNSCALER

Julia Borisova, Dmitry Morozov, Dmitry Gilemkhanov, Nikolay O. Nikitin
AI Institute, ITMO University, Saint-Petersburg, Russia
{jul.borisova, dmitmorozov, dmitryglhf, nnikitin}@itmo.ru

ABSTRACT

This paper presents an approach for Arctic sea ice concentration correction and downscaling based on multi-sensor fusion that is applied only during the training stage. While conventional downscaling methods primarily enhance spatial resolution, the proposed approach also improves physical consistency by fusing the widely used OSISAF sea ice concentration dataset with the high-resolution multi-sensor-corrected MASAM2 product. This synthesis not only increases spatial resolution from 25 km to 4 km, but also yields more realistic ice patterns, as validated by a mean absolute error (MAE) of 0.009 and high structural similarity (SSIM) scores. Comparisons with classical downscaling techniques and manual product hybridization confirm the superior performance of our model. The proposed solution has strong potential to improve sea ice forecasting and generate high-resolution historical datasets. Code and weights are provided on GitHub[1].

1 INTRODUCTION

Sea ice concentration (SIC) - the fractional area covered by ice within a grid cell - is the most important variable for monitoring and predicting Arctic conditions. Satellite-based passive microwave observations have provided continuous SIC estimates since 1978, forming the backbone of climate data records (Lavergne et al., 2019). However, these products face an inherent trade-off between temporal coverage and spatial resolution. Long-term climate data records derived from SMMR, SSM/I, and SSMIS instruments offer over four decades of observations but have relatively coarse spatial resolution (approximately 25 km). In contrast, modern multisensor products combining various satellite sources can achieve higher spatial resolution (4 km) but are available only for the past few decades. It causes a challenge for effective sea ice forecasting due to the uneven quality of data (Ran et al., 2026).

This resolution gap poses challenges for applications requiring both long historical records and fine-scale spatial detail. Traditional interpolation methods, such as bilinear, bicubic, and nearest-neighbor approaches, can increase nominal resolution but cannot recover sub-grid information absent in the original data. For instance, mesoscale ice features and edge dynamics that fall below the coarse resolution threshold remain unresolved (Kvanum et al., 2025). Similar issues are faced by the weight-based approach for downscaling (Ahn et al., 2014).

Deep learning approaches offer a promising alternative for spatial downscaling of climate data. Super-resolution techniques, originally developed for image enhancement in computer vision, have been successfully adapted for climate applications, including precipitation (Chiang et al., 2024; Lin et al., 2023), temperature (Jha et al., 2025), and general climate variables (Serifi et al., 2021). These methods learn mappings from low-resolution to high-resolution representations, potentially capturing physical relationships that enable reconstruction of fine-scale features. U-Net architectures (Ronneberger et al., 2015) have proven particularly effective for such tasks due to their ability to preserve spatial context through skip connections (Andersson et al., 2021; Palerme et al., 2024). For sea ice applications specifically, deep learning has demonstrated success in forecasting SIC (Andersson et al., 2021; Li et al., 2024) and improving forecast skill through post-processing (Palerme

[1]https://github.com/ITMO-NSS-team/ML4RS_2026_arctic_downscale

et al., 2024; Kvanum et al., 2025) or using a downscaling stage as a part of a forecasting model (Xu et al., 2025). Some works have explored the applicability of GANs (Rocha et al., 2025) and attention-based architectures (He et al., 2025) for super-resolution of sea ice concentration, but they considered a single-source setup. We can conclude that the application of learned downscaling to extend high-resolution SIC records back in time using different data sources remains underexplored.

In this work, we present a deep learning-based approach that **enhances the spatial resolution** of long-term SIC observations and improves **reproduction of natural physics patterns** through fusion with additional high-quality data. Using paired observations from a coarse-resolution climate data record (OSISAF - approximately 25 km) and a high-resolution multisensor product (MASAM2 - 4 km) during their overlapping period, we train a U-Net-based model to learn the low-to-high-resolution mapping. Our objectives are follows: (1) to evaluate whether deep learning downscaling provides meaningful improvements over classical interpolation methods for SIC data; (2) to compare physical coherence of high-resolution fields produced with our approach, classical approach and manual multisensor hybridization; (3) to assess the feasibility of reconstructing high-resolution SIC fields for the historical period before modern multisensor products became available.

2 Improvement of sea ice concentration data

2.1 Datasets

As a case study, we utilize two sea ice concentration products that differ substantially in spatial resolution and temporal coverage, enabling a paired training approach for learned downscaling:

OSI SAF: 25 km. The EUMETSAT Ocean and Sea Ice Satellite Application Facility (OSI SAF) provides the Global Sea Ice Concentration Climate Data Record (OSI-450-a) and its interim extension (OSI-430-a), covering the period from *October 1978 to present* (Lavergne et al., 2019). This product is derived from passive microwave brightness temperatures measured by SMMR, SSM/I, and SSMIS instruments aboard various satellites. Sea ice concentrations are computed algorithmically using dynamic tie points that adapt to evolving surface characteristics and inter-sensor calibration differences. The data are provided on a polar stereographic grid at approximately 25 km resolution (grid cell size 432×432 pixels for the Arctic domain). Key advantages of this dataset include its long and stable time series, quantitative uncertainty estimates for each grid cell, and atmospheric correction using ERA5 reanalysis data. The OSI SAF represents the widely used reference for sea ice monitoring and climate studies.

MASAM2: 4 km. The MASIE-AMSR2 (MASAM2) product provides high-resolution daily sea ice concentration estimates at 4 km grid cell size (Fetterer et al., 2023). This product blends two complementary data sources: the Multisensor Analyzed Sea Ice Extent (MASIE) product, which provides ice extent information at 4 km resolution based on operational ice analysis incorporating synthetic aperture radar, infrared, visible imagery, and in situ observations; and sea ice concentration from the Advanced Microwave Scanning Radiometer 2 (AMSR2) at 10 km resolution. By combining the spatial precision of MASIE ice edge detection with AMSR2 concentration gradients, MASAM2 achieves a high-resolution concentration product (grid size 2550×2100 pixels for the Arctic domain) suitable for operational forecast model initialization. The dataset is available *from July 2012 to present*.

Downscaling Strategy. For model training, we construct paired samples by matching daily observations from both products over their common temporal coverage (July 2012 - present). The OSI SAF data serve as low-resolution input, while the corresponding MASAM2 fields provide high-resolution targets. This configuration enables the model to learn the mapping from coarse passive microwave observations to the finer-scale patterns captured by the multisensor analysis. The substantial resolution ratio (approximately $6\times$ in each spatial dimension) presents both an opportunity for meaningful enhancement and a challenge for accurate reconstruction of sub-grid features.

The two products use different native projections: OSI SAF uses a Lambert Azimuthal Equal Area (LAEA) projection centered on the North Pole, while MASAM2 uses a polar stereographic projection following the EASE-Grid 2.0 North specification. Thus, the direct pairing of these two datasets inherently requires reprojection. We allow the neural network to learn this reprojection transformation alongside super-resolution, enabling a native neural transition between the two product formats.

2.2 Models

Proposed approach. We implemented a lightweight U-Net architecture specifically optimized for super-resolution of sea ice concentration (SIC) data with an approximate scale ratio of 6×. The model transforms low-resolution inputs (432×432 pixels, OSISAF product) into high-resolution outputs (2100×2550 pixels, MASAM2 product). The architecture of the model is presented in Figure 1.

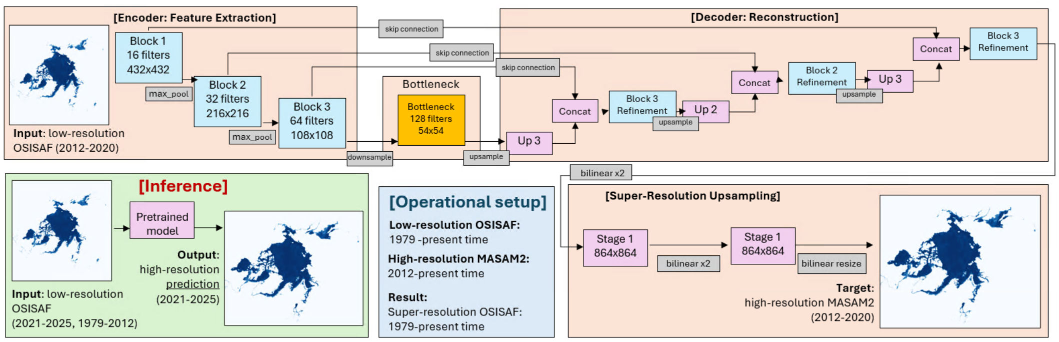

Figure 1: Scheme of proposed approach with details of implemented U-Net architecture. Train and inference setups are used for experiments, operational demonstrate the real usage scenario.

To achieve the target resolution of 2100×2550, a multi-stage upsampling strategy is applied. Firstly, two sequential bilinear upsampling stages with scale factor ×2 (reaching 1728×1728). Secondly, final precise resizing to 2100×2550 via Upsample with bilinear interpolation. Large convolutional kernels (7×7) replace standard 3×3 kernels to capture broader spatial context with fewer layers. Reduced channel counts (16–128 filters) minimize GPU memory consumption while maintaining representational capacity. The model was trained using L1 loss (Mean Absolute Error), the Adam optimizer with an initial learning rate of 0.001, and dynamic learning rate scheduling via ReduceLROnPlateau (factor 0.5, patience 5 epochs) triggered by validation metric stagnation.

Baselines. We used three classical interpolation methods as baselines for comparison with the proposed approach. *Bilinear interpolation* produces smooth outputs, but tends to blur sharp boundaries such as the sea ice edge. *Bicubic interpolation* preserves smooth gradients better than bilinear interpolation, but cannot recover sub-grid structures absent in the source data and may introduce ringing artifacts near abrupt transitions. *Nearest-neighbor* interpolation preserves the original concentration values without distortion, but does not produce smooth transitions between regions of differing ice concentration, resulting in a blocky appearance.

Manual hybridization. For comparative analysis, we implement a manual hybridization method analogous to the approach described by (Nikitin et al., 2025) for OSISAF-MASIE data fusion. The method leverages the complementary characteristics of the source products: the low-resolution product provides the full-range concentration values, while the high-resolution product defines the precise ice edge. The hybrid field is generated by using the ice concentration values from the low-resolution product and the ice edge mask (e.g., concentration $\geq$ 0.15) from the high-resolution product to correct spurious low-concentration artifacts. This simple, non-trainable baseline serves to benchmark the performance gains achievable by more sophisticated, learnable super-resolution models against an established manual fusion technique.

3 Results and Discussion

Averaged quality metrics for train (2012-2020, $\sim$ 2920 samples), validation (2021-2022, $\sim$ 730 samples), and test (2023-2025, $\sim$ 1095 samples) samples are presented in Table 1. Metrics demonstrate that the proposed approach achieves the best quality compared to classical interpolation methods. The high performance of the implemented architecture confirms its sufficiency for solving the given problem. Also, we analyzed comparative visualization for low and high-resolution fields. Figure 2a) demonstrates a sample with successful restoration of the missing ice edge after using the proposed downscaling model. Summer images (Figure 2b) demonstrate the advantage of the proposed method over a manual hybrid.

Table 1: Performance comparison against MASAM2[2]

Method	Split	BACC	IIEE ($\times 10^5$)	MAE	PSNR	SSIM
Proposed	Train	**0.923 ± 0.075**	**0.436 ± 0.443**	**0.008 ± 0.002**	**23.81 ± 1.32**	**0.973 ± 0.017**
	Val	**0.906 ± 0.059**	**0.509 ± 0.211**	**0.009 ± 0.002**	**23.18 ± 1.17**	**0.966 ± 0.018**
	Test	**0.899 ± 0.072**	**0.514 ± 0.309**	**0.009 ± 0.002**	**23.20 ± 1.46**	**0.963 ± 0.026**
Bilinear	Train	0.318 ± 0.063	4.15 ± 1.64	0.070 ± 0.009	12.52 ± 0.72	0.597 ± 0.016
	Val	0.331 ± 0.061	4.06 ± 1.62	0.068 ± 0.028	13.18 ± 2.44	0.612 ± 0.051
	Test	0.321 ± 0.060	3.96 ± 1.63	0.067 ± 0.028	13.33 ± 2.56	0.607 ± 0.047
Bicubic	Train	0.316 ± 0.062	4.16 ± 1.64	0.071 ± 0.010	12.41 ± 0.73	0.591 ± 0.018
	Val	0.329 ± 0.060	4.07 ± 1.62	0.069 ± 0.028	13.08 ± 2.45	0.607 ± 0.051
	Test	0.319 ± 0.059	3.97 ± 1.63	0.068 ± 0.029	13.22 ± 2.58	0.602 ± 0.048
Nearest	Train	0.314 ± 0.060	4.16 ± 1.63	0.070 ± 0.010	12.38 ± 0.77	0.589 ± 0.018
	Val	0.327 ± 0.058	4.08 ± 1.61	0.068 ± 0.028	13.04 ± 2.45	0.605 ± 0.051
	Test	0.317 ± 0.058	3.98 ± 1.62	0.067 ± 0.028	13.19 ± 2.58	0.599 ± 0.048

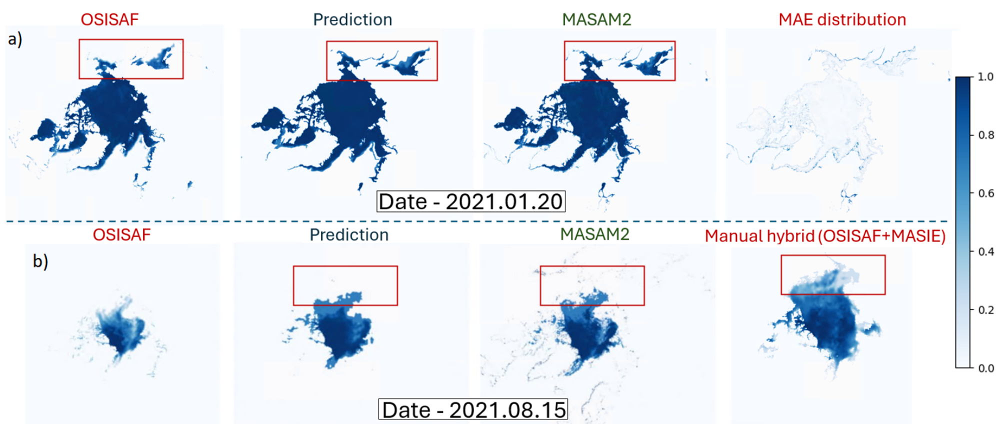

Figure 2: Comparison of low and high resolution images a) winter downscaling result; (b) summer downscaling result and manual hybrid. The frame is on the area of interest with a refined ice edge.

4 Conclusion

This study demonstrates that a deep learning approach based on a U-Net architecture can effectively downscale coarse-resolution (25 km) Arctic sea ice concentration data to high resolution (4 km), outperforming classical interpolation methods and a manual hybridization technique. The model successfully reconstructs physically realistic fine-scale features, such as the ice edge, while achieving superior validation metrics (MAE: 0.009, SSIM: 0.963). This approach enables the generation of long-term, high-resolution SIC datasets, offering significant potential for improving sea ice forecasting, local-scale modeling, and historical climate analysis.

5 Acknowledgment

This work supported by the Ministry of Economic Development of the Russian Federation (IGK 000000C313925P4C0002), agreement No139-15-2025-010.

[2]Mean $\pm$ standard deviation. BACC: Balanced Accuracy, IIEE: Integrated Intensity Error, MAE: Mean Absolute Error, RMSE: Root Mean Square Error, PSNR: Peak Signal-to-Noise Ratio, SSIM: Structural Similarity Index.

REFERENCES

Jihye Ahn, Sungwook Hong, Jaeil Cho, and Yang-Won Lee. Downscaling of amsr2 sea ice concentration using a weighting scheme derived from modis sea ice cover product. *Korean Journal of Remote Sensing*, 30(5):687–701, 2014.

Tom Andersson, Scott Hosking, María Pérez-Ortiz, Brooks Paige, Andrew Elliott, Chris Russell, Stephen Law, Dani Jones, Jeremy Wilkinson, Tony Phillips, James Byrne, Steffen Tietsche, Beena Sarojini, Eduardo Blanchard-Wrigglesworth, Yevgeny Aksenov, Rod Downie, and Emily Shuckburgh. Seasonal arctic sea ice forecasting with probabilistic deep learning. *Nature Communications*, 12, 08 2021. doi: 10.1038/s41467-021-25257-4.

Chia-Hao Chiang, Zheng-Han Huang, Liwen Liu, Hsin-Chien Liang, Yi-Chi Wang, Wan-Ling Tseng, Chao Wang, Che-Ta Chen, and Ko-Chih Wang. Climate downscaling: A deep-learning based super-resolution model of precipitation data with attention block and skip connections. 2024. URL `https://arxiv.org/abs/2403.17847`.

Florence Fetterer, James Scott Stewart, and Walt N Meier. Masam2: Daily 4 km arctic sea ice concentration, version 2, 2023. URL `https://nsidc.org/data/G10005/versions/2`.

Jianxin He, Shuo Yang, Haoyu Wang, Wanshou Liu, and Xiong Deng. Enhancing polar sea ice estimation: Deep saru-net for spatiotemporal super-resolution approach. *Remote Sensing*, 17(23): 3839, 2025.

Shailesh Kumar Jha, Vivek Gupta, Priyank J. Sharma, Anurag Mishra, and Saksham Joshi. Deep learning super-resolution for temperature data downscaling: a comprehensive study using residual networks. *Frontiers in Climate*, Volume 7 - 2025, 2025. ISSN 2624-9553. doi: 10.3389/fclim.2025.1572428. URL `https://www.frontiersin.org/journals/climate/articles/10.3389/fclim.2025.1572428`.

A. F. Kvanum, C. Palerme, M. Müller, J. Rabault, and N. Hughes. Developing a deep learning forecasting system for short-term and high-resolution prediction of sea ice concentration. *The Cryosphere*, 19(10):4149–4166, 2025. doi: 10.5194/tc-19-4149-2025. URL `https://tc.copernicus.org/articles/19/4149/2025/`.

T. Lavergne, A. M. Sørensen, S. Kern, R. Tonboe, D. Notz, S. Aaboe, L. Bell, G. Dybkjær, S. Eastwood, C. Gabarro, G. Heygster, M. A. Killie, M. Brandt Kreiner, J. Lavelle, R. Saldo, S. Sandven, and L. T. Pedersen. Version 2 of the eumetsat osi saf and esa cci sea-ice concentration climate data records. *The Cryosphere*, 13(1):49–78, 2019. doi: 10.5194/tc-13-49-2019. URL `https://tc.copernicus.org/articles/13/49/2019/`.

Yang Li, Yubao Qiu, Guoqiang Jia, Shuwen Yu, Yixiao Zhang, Lin Huang, and Matti Leppäranta. An explainable deep learning model for daily sea ice concentration forecast. *IEEE Transactions on Geoscience and Remote Sensing*, 62:1–17, 2024. doi: 10.1109/TGRS.2024.3386930.

Hai Lin, Jianping Tang, Shuyu Wang, Shuguang Wang, and Guangtao Dong. Deep learning downscaled high-resolution daily near surface meteorological datasets over east asia. *Scientific Data*, 10, 12 2023. doi: 10.1038/s41597-023-02805-9.

N. O. Nikitin, Yu. I. Borisova, Ya. V. Aksenkin, K. Bashkova, E. I. Lutsenko, A. V. Kalyuzhnaya, D. O. Yakimushkin, A. M. Kotilevskaya, T. N. Vertash, A. A. Kolubakin, E. S. Bagoryan, and A. V. Bukhanovsky. Prediction of ice conditions to support economic activity in the Russian Arctic seas using deep learning methods. *Arctic: Ecology and Economy*, 15(1):119–130, 2025. ISSN 2223-4594. doi: 10.25283/2223-4594-2025-1-119-130. In Russian.

C. Palerme, T. Lavergne, J. Rusin, A. Melsom, J. Brajard, A. F. Kvanum, A. Macdonald Sørensen, L. Bertino, and M. Müller. Improving short-term sea ice concentration forecasts using deep learning. *The Cryosphere*, 18(4):2161–2176, 2024. doi: 10.5194/tc-18-2161-2024. URL `https://tc.copernicus.org/articles/18/2161/2024/`.

Junlin Ran, Weimin Zhang, and Yi Yu. Research progress of deep learning in sea ice prediction. *Remote Sensing*, 18(3):419, 2026.

ML Rocha, AH Lynch, and KJ Bergen. Enhancing sea ice concentration resolution in a northern sea route strait using a generative adversarial network. *Journal of Geophysical Research: Machine Learning and Computation*, 2(1):e2024JH000281, 2025.

Olaf Ronneberger, Philipp Fischer, and Thomas Brox. U-net: Convolutional networks for biomedical image segmentation. In Nassir Navab, Joachim Hornegger, William M. Wells, and Alejandro F. Frangi (eds.), *Medical Image Computing and Computer-Assisted Intervention – MICCAI 2015*, pp. 234–241, Cham, 2015. Springer International Publishing. ISBN 978-3-319-24574-4.

Agon Serifi, Tobias Günther, and Nikolina Ban. Spatio-temporal downscaling of climate data using convolutional and error-predicting neural networks. *Frontiers in Climate*, Volume 3 - 2021, 2021. ISSN 2624-9553. doi: 10.3389/fclim.2021.656479. URL https://www.frontiersin.org/journals/climate/articles/10.3389/fclim.2021.656479.

Jingyi Xu, Siwei Tu, Weidong Yang, Ben Fei, Shuhao Li, Keyi Liu, Yeqi Luo, Lipeng Ma, and Lei Bai. Icediff: High resolution and high-quality arctic sea ice forecasting with generative diffusion prior. In *Proceedings of the Computer Vision and Pattern Recognition Conference*, pp. 10567–10576, 2025.